Electronic Supplementary Material (ESI) for Materials Chemistry Frontiers.

Supplementary Information

The supercapacitor electrode properties and energy storage mechanism of binary transition metal sulfide $MnCo_2S_4$ compared with oxide $MnCo_2O_4$ studied using *in situ* quick X-ray absorption spectroscopy

Su-Yang Hsu[1], Feng-Hao Hsu[1,#], Jeng-Lung Chen[1], Yu-Song Cheng[1], Jin-Ming Chen[1,*] and Kueih-Tzu Lu[1,*]

[1]National Synchrotron Radiation Research Center, Hsinchu 30076, Taiwan

*E-mail: jmchen@nsrrc.org.tw (J. M. Chen), ktlu@nsrrc.org.tw (K. T. Lu)

[#] Contributed equally to this work with the first author: S. Y. Hsu.

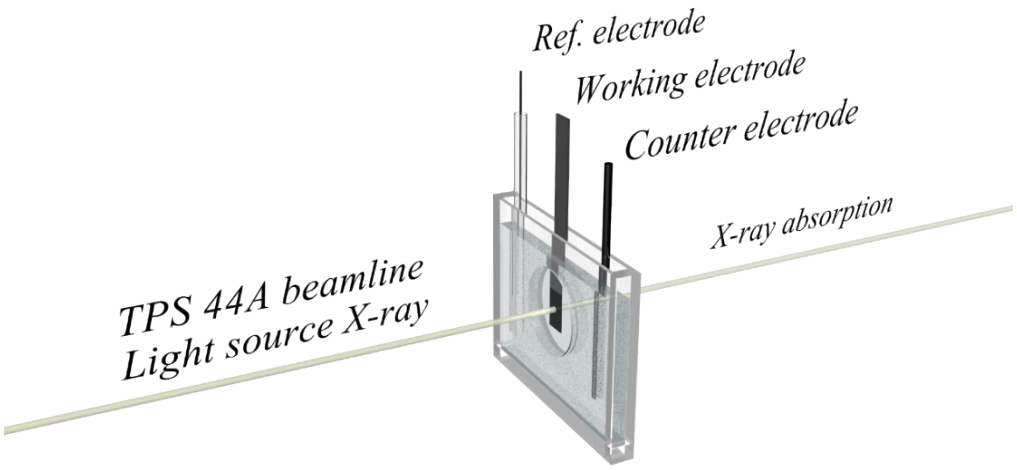

Fig. S1. The illustration of *in situ* XAS electrochemical reaction cell.

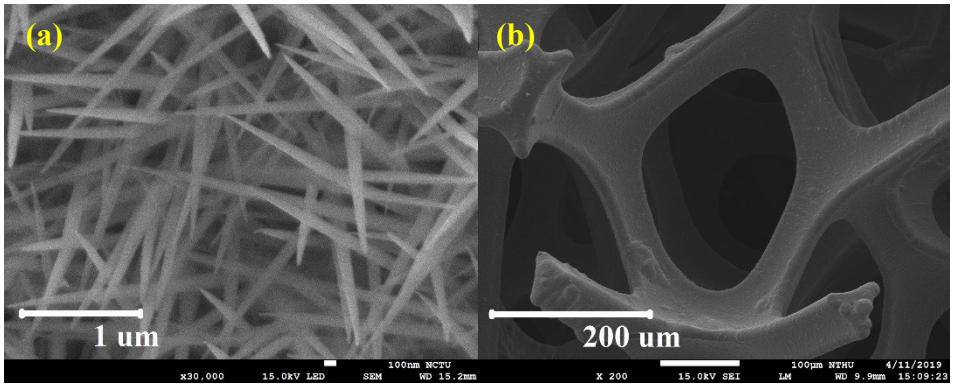

Fig. S2. FE-SEM images of (a) a Mn-Co precursor on a Ni foam and (b) a pristine Ni foam.

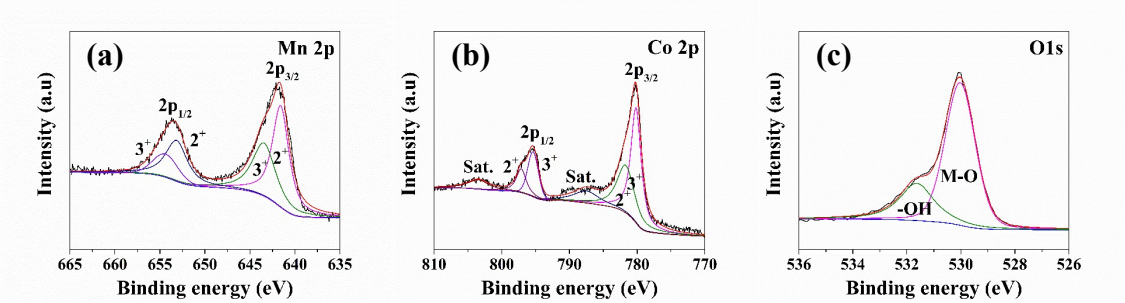

Fig. S3. XPS spectra and the corresponding fitted curve of (a) Mn 2p, (b) Co 2p and (c) O 1s in the MCO/NF electrode as prepared.

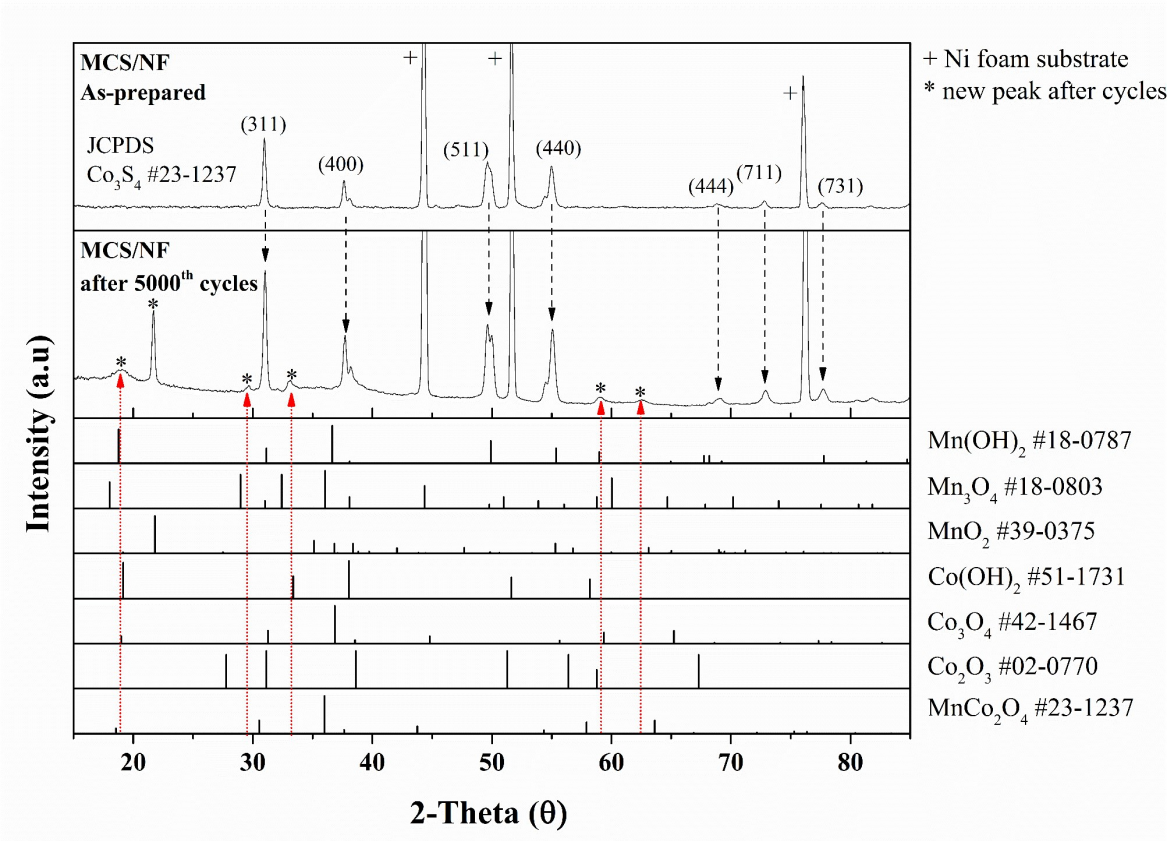

Fig. S4. The synchrotron-based XRD patterns of MCS/NF electrode of as prepared and after 5000th charge/discharge cycles compared with MCO, Mn oxide/hydroxide and Co oxide/hydroxide JCPDS cards for comparison.

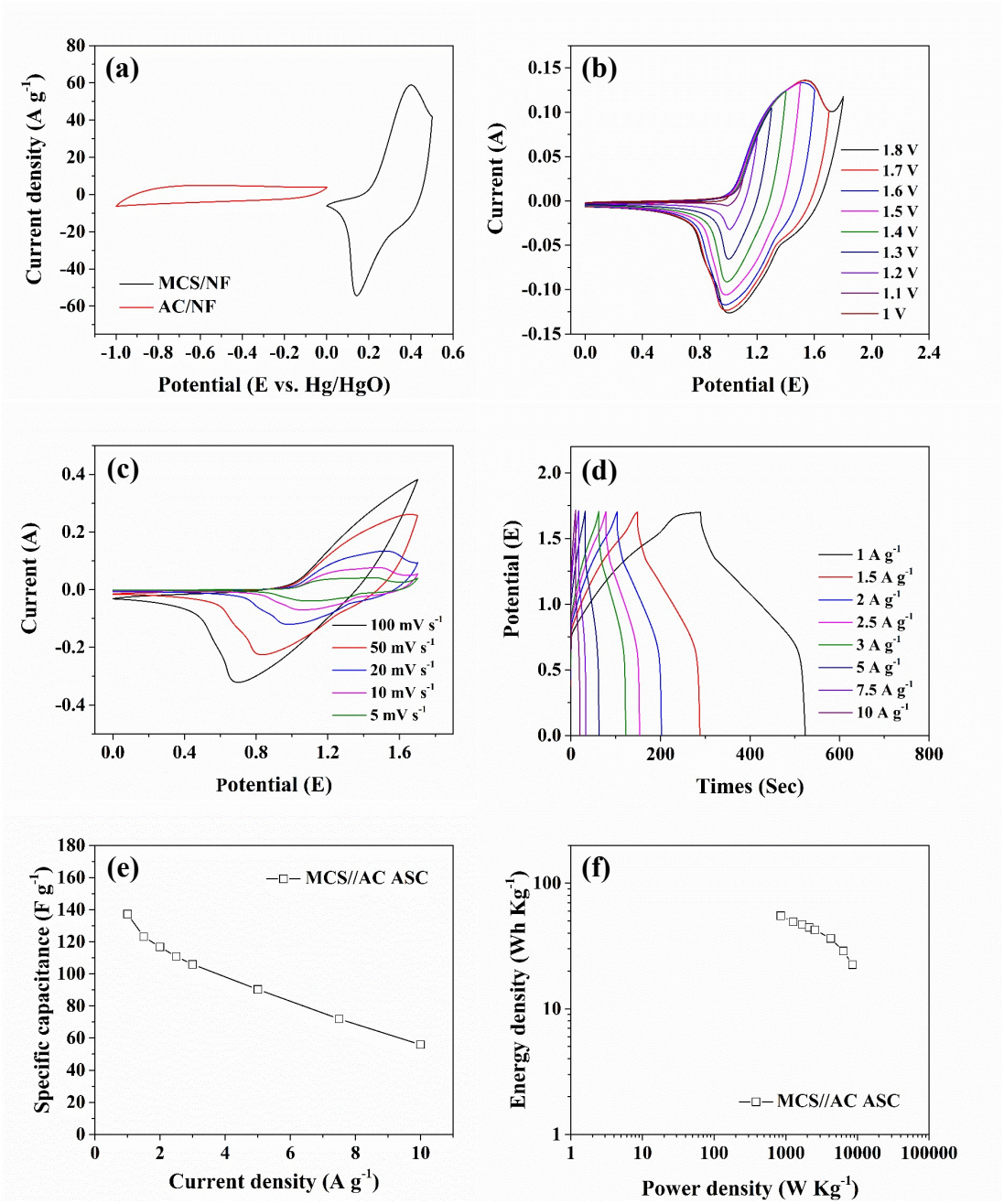

Fig. S5. Electrochemical performance of MCS//AC ASC in KOH aqueous electrolyte, (a) CV curves at scan rate 50 mV s^{-1} of the MCS/NF and AC/NF electrodes. (b) CV curves of MCS//AC ASC at various potential windows from 1 to 1.8 V at scan rate 50 mV s^{-1}. (c) CV curves of MCS//AC ASC at various scan rates. (d) GCD curves of MCS//AC ASC at varied current densities. (e) Specific capacity versus current density of MCS//AC ASC. (f) Ragone plot of MCS//AC ASC.

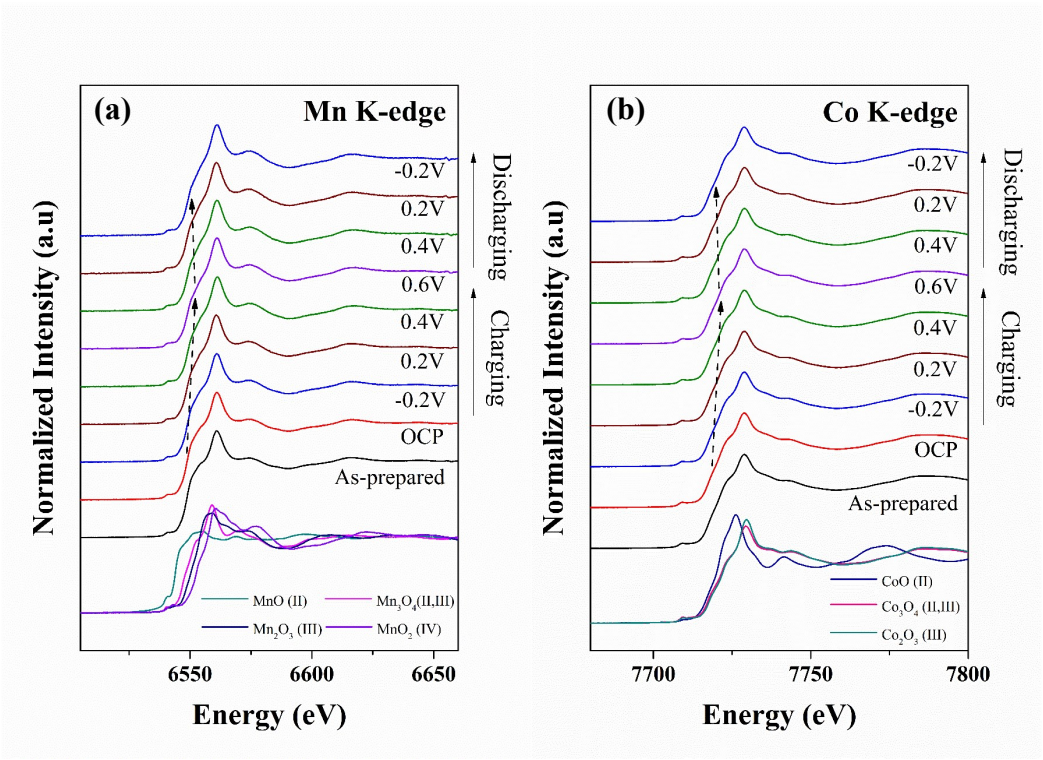

Fig. S6. XANES spectra of a MCO sample *in situ* at various operating potentials at the (a) Mn K-edge and (b) Co K-edge.

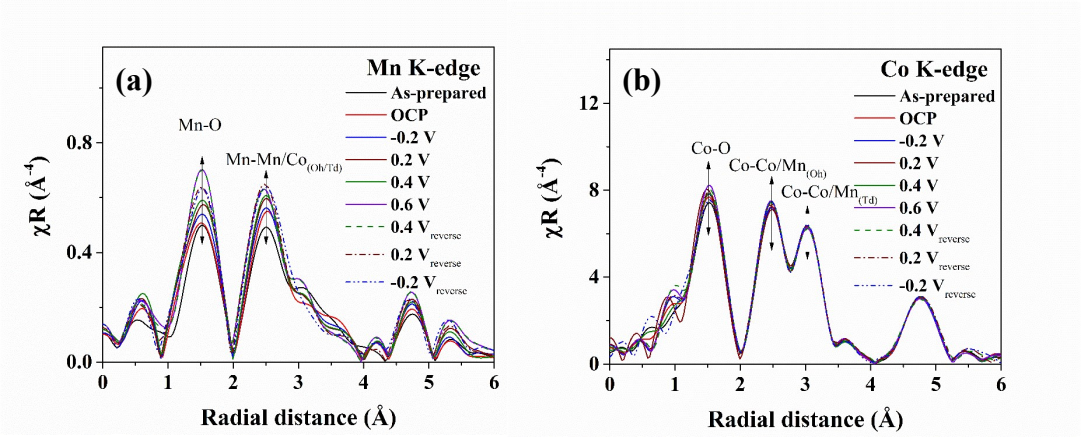

Fig. S7. Radial distribution function (RDF) deduced from the Fourier transforms of k^3-weighted EXAFS spectra of a MCO sample at various operating potentials at the (a) Mn K-edge and (b) Co K-edge during charging and discharging

Table S1. Electrochemical performance of $MnCo_2S_4$ compared with previous reports

Electrode Material	Electrolyte	Capacity / mAh cm^{-2}	Cycle stability	Reference
$NiCo_2S_4$@NiCu−LDH[ab]	3 M KOH	0.632 at 2 mA cm^{-2}	74% after 3000 cycle	1
$Cu_{0.5}Co_{0.5}$-P@$Ni(OH)_2$[b]	2 M KOH	0.392 at 2 mA cm^{-2}	NA	2
$NiMoO_4$	3 M KOH	0.33 at 1 mA cm^{-2}	85.1% after 10K cycle	3
NiCo LDH[a]	2 M KOH	0.19 at 0.5 mA cm^{-2}	89% after 10K cycle	4
$CoMoO_4$@$NiWO_4$[b]	6 M KOH	0.464 at 5 mA cm^{-2}	92.5% after 3000 cycle	5
$MnCo_2S_4$	6 M KOH	1.17 at 3 mA cm^{-2}	89.93% after 5000 cycle	this work

[a] Layered Double Hydroxides (LDH)

[b] core-shell structure

References

1. J. Huang, J. Xie, L. Wang, J. Zhang, P. Wang, P. Sun, Z. Yao and Y. Yang, Boosted Electrochemical Performance of Honeycomb-Like NiCu–LDH Nanosheets Anchoring on $NiCo_2S_4$ Nanotube Arrays for Flexible Solid-State Hybrid Supercapacitors, *Energy Fuels*, 2020, **34**, 13157-13166.

2. X. Li, J. Huang, L. Wang, J. Zhang, S. Song, G. Li, P. Wang, P. Sun and Y. Yang, Hierarchical honeycomb-like networks of CuCo–P@$Ni(OH)_2$ nanosheet arrays enabling high-performance hybrid supercapacitors, *J. Alloys Compd.*, 2020, **838**, 155626.

3. K. A. Owusu, L. Qu, J. Li, Z. Wang, K. Zhao, C. Yang, K. M. Hercule, C. Lin, C. Shi, Q. Wei, L. Zhou and L. Mai, Low-crystalline iron oxide hydroxide nanoparticle anode for high-performance supercapacitors, *Nat. Commun.*, 2017, **8**, 14264.

4. K.-N. Kang, A. Ramadoss, J.-W. Min, J.-C. Yoon, D. Lee, S. J. Kang and J.-H. Jang, Wire-Shaped 3D-Hybrid Supercapacitors as Substitutes for Batteries, *Nanomicro Lett*, 2020, **12**, 28.

5. F. H. Hsu, S. Y. Hsu, C. W. Pao, J. L. Chen, C. L. Chen, J. M. Chen and K. T. Lu, Electrochemical properties and mechanism of $CoMoO_4$@$NiWO_4$ core–shell nanoplates for high-performance supercapacitor electrode application studied

via in situ X-ray absorption spectroscopy, *Nanoscale*, 2020, **12**, 13388-13397.